Supplementary Information

A strain-sensitive neuromorphic device emulating mechanoreception for different skin sensitivities

Shubhanshi Mishra†[a] , Bhupesh Yadav†[a] , Giridhar U Kulkarni [a]

[a] *Chemistry & Physics of Materials Unit, Jawaharlal Nehru Centre for Advanced Scientific Research, Jakkur P. O., Bangalore-560064, India.*

corresponding author

E-mail: kulkarni@jncasr.ac.in

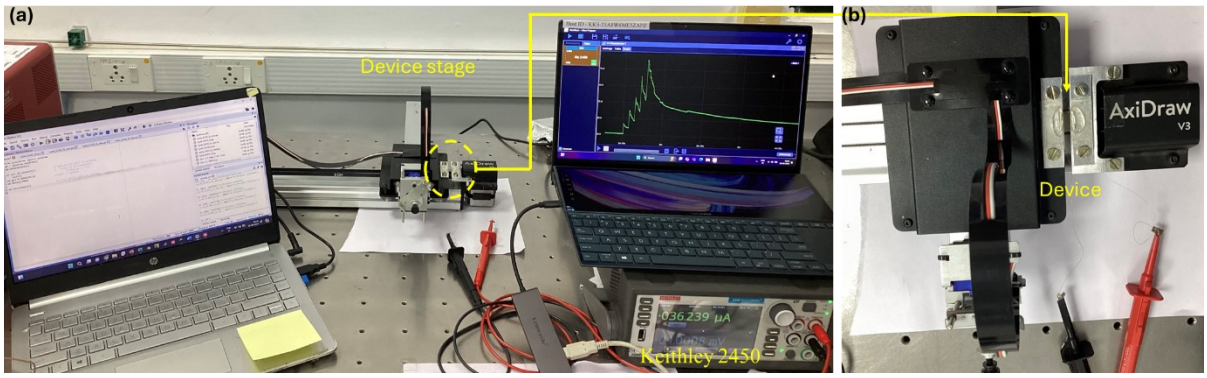

Fig. S1 (a) Photograph of the experimental setup. The device was mounted on a stage with automated translational movement controlled through Python programming. The resistance change in the device, resulting from the applied strain due to the translational motion, was continuously monitored under a bias voltage using a Keithley 2450 source meter. (b) Enlarged image of the device.

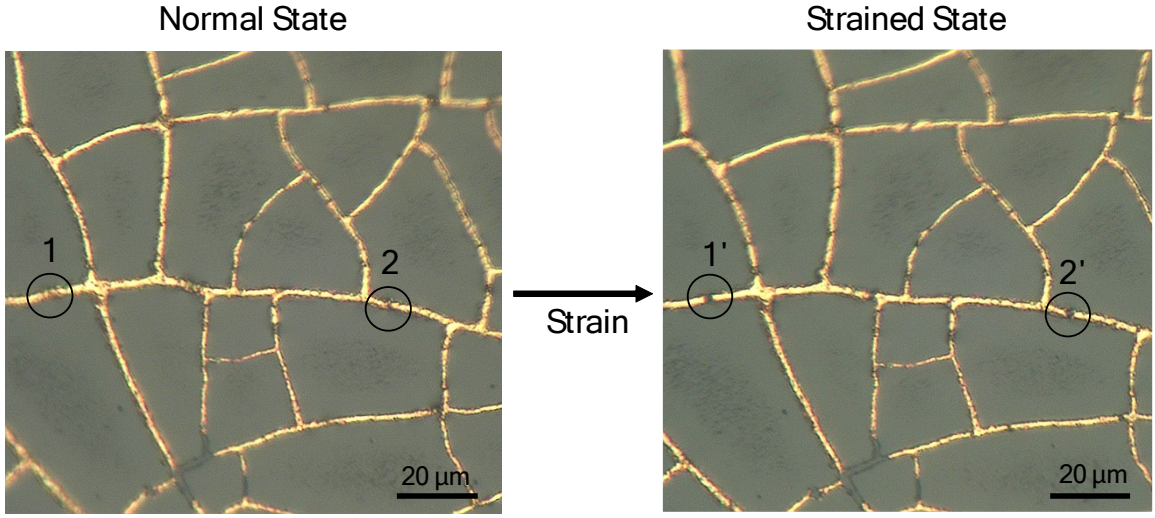

Fig. S2 Microscopy images of the device in normal and strained state showing the formation of gaps at 1 and 2 (normal state) and 1' and 2' (strained state) on the application of strain.

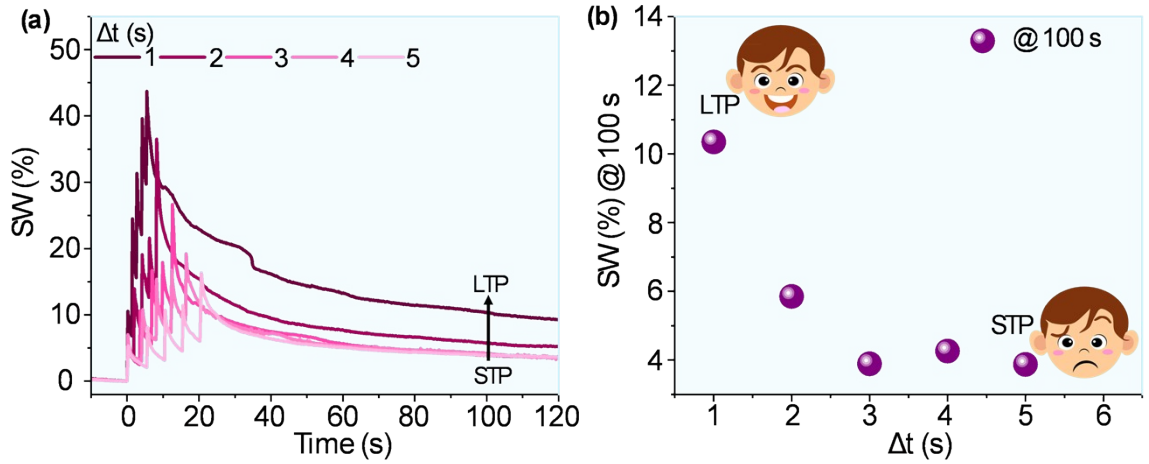

Fig. S3 (a) Variation of SW of the device with time at different Δt depicting spike rate dependent plasticity (SRDP) (D2, Δx, 16 μm, and ε, 0.27%). (b) The values indicating the change in SW at 100 s after pulsing were observed across five different intervals, depicting the transition from STP to LTP with a decrease in time interval.

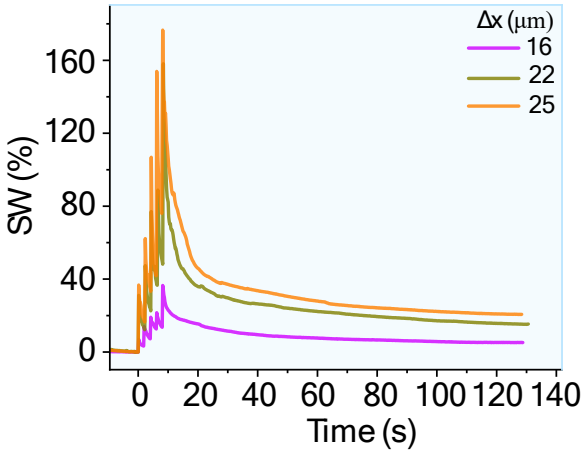

Fig. S4 Variation of SW of the device with time at different Δx depicting Spike amplitude dependent plasticity (SADP) (D2, C:B, 1:10 and Δt, 2s).

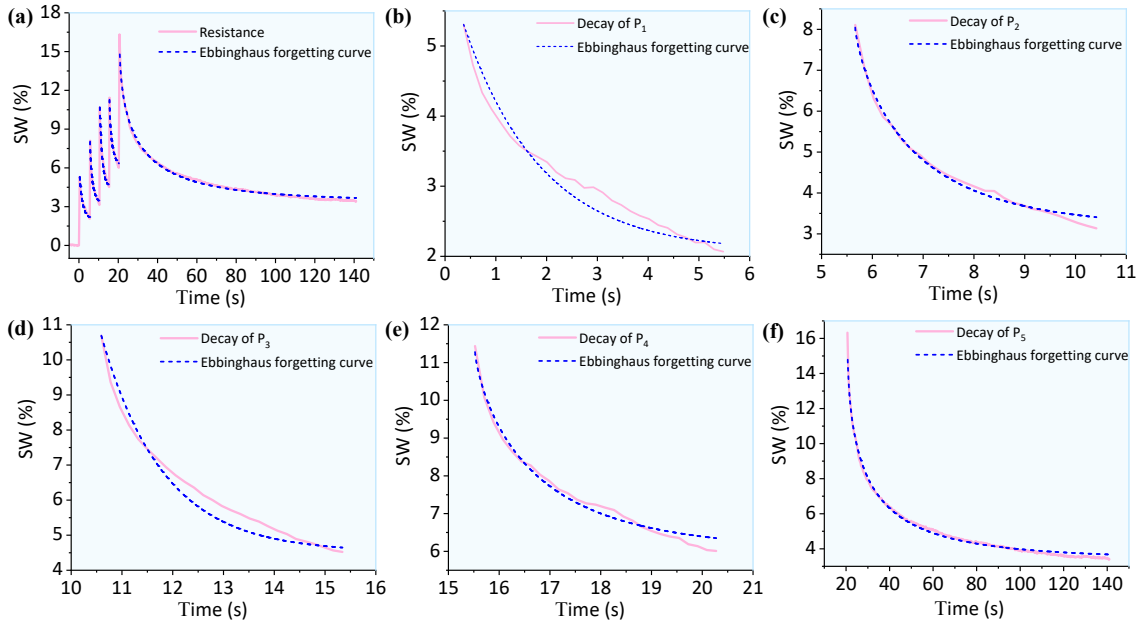

Fig. S5 (a) SW variation of the device D2 with time after the successive application of five displacement pulses of 16 µm magnitude at Δt as 5 s. (b-f) Decay of peak P_1, P_2, P_3, P_4, and P_5 fitted with Ebbinghaus forgetting curve.

To evaluate the yield and performance of the device across different batches, we fabricated five similar devices with a curing agent-to-base (C:B) ratio of 1:10 (Di, Dii, Diii, Div, and Dv). Each device was subjected to five consecutive displacement pulses of 16 µm (ε, 0.27%), with time intervals of 2 and 4 seconds, leading to an increase in strain with each applied pulse and a corresponding rise in the SW (Fig. S6). After the displacement pulses were removed, the SW gradually decayed due to the flexible PDMS matrix underneath. As shown in Fig. S6, at a strain (ε) of 0.27% and a time interval (Δt) of 2 seconds, the SW enhancement was approximately 75% for Di, 55% for Dii, 8% for Diii, 30% for Div, and 35% for Dv. All five devices exhibited a similar pattern of SW enhancement and decay, with slight variations in the SW enhancement range, which were influenced by the fill factor of the Au wire network on the PDMS.

Similar analysis was also performed at another strain value (ε as 0.36% and Δx, 22 µm), showing higher enhancement in SW due to higher strain while preserving the enhancement and decay patterns. (Fig. S7)

Additionally, the A_2/A_1 (%) was calculated for all the curves in Fig. S6 (a-e), and Fig. S7 (a-e), and their mean is plotted for each device. Despite the variation in the SW range, all the devices exhibited a remarkable A_2/A_1 value of ~200%, demonstrating the strong PPF effect in the devices (Fig. S8). All these analyses certify the reliability of these devices among different batches.

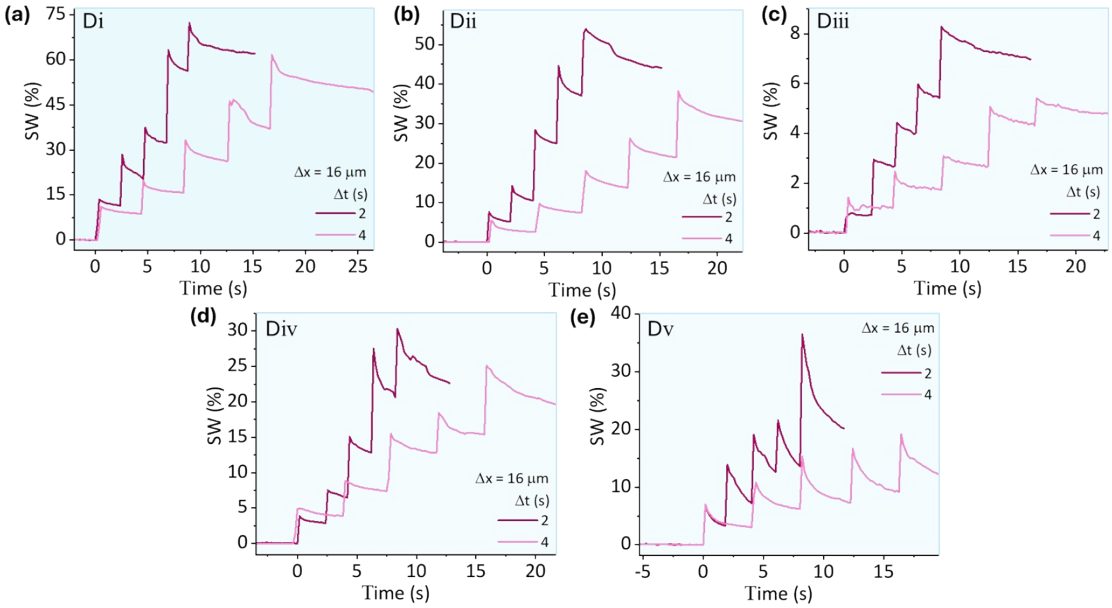

Fig. S6 Change in SW of five devices Di (a), Dii(b), Diii(c), Div(d), and Dv(e) when displacement pulses are applied at varying time intervals (Δt, 2 and 4 s) at a strain of 0.27% (Δx, 16 μm).

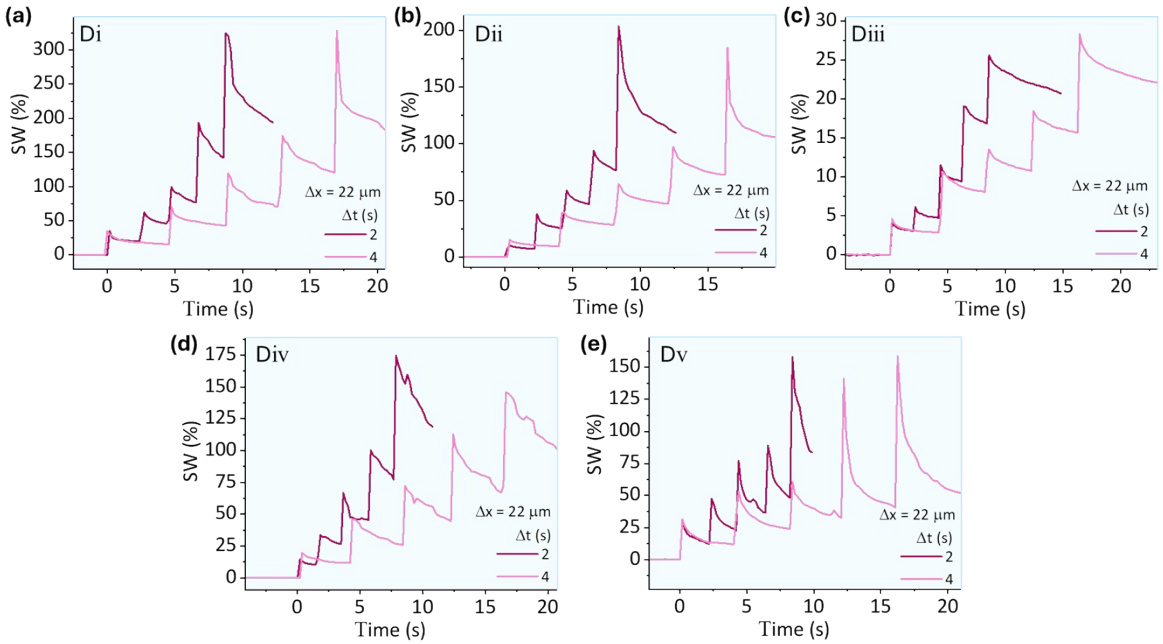

Fig. S7 Change in SW of Di(a), Dii(b), Diii(c), Div(d), and Dv(e) when displacement pulses are applied at varying time intervals (Δt, 2 and 4 s) at a strain of 0.36% (Δx, 22 μm).

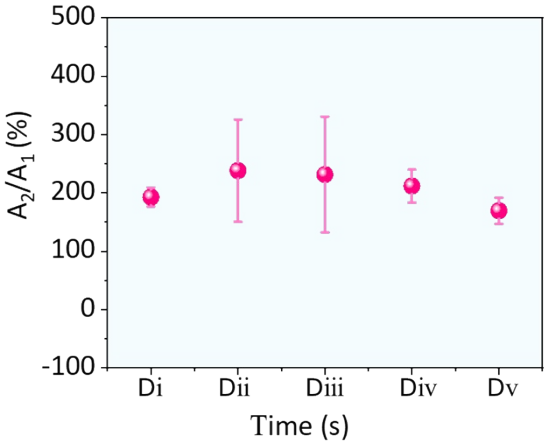

Fig S8. Change in PPF index (A_2/A_1) (%) of Di, Dii, Diii, Div, and Dv when displacement pulses of 16 and 22 µm are applied at varying time intervals (Δt, 2 and 4 s).

We conducted a comprehensive cyclic stability study across varying strain levels (0.27%, 0.31%, and 0.36%), as illustrated in Fig. S9. The results demonstrate that the change in resistance remains consistently repeatable across 155 cycles, indicating the robustness of the device under repeated mechanical stress.

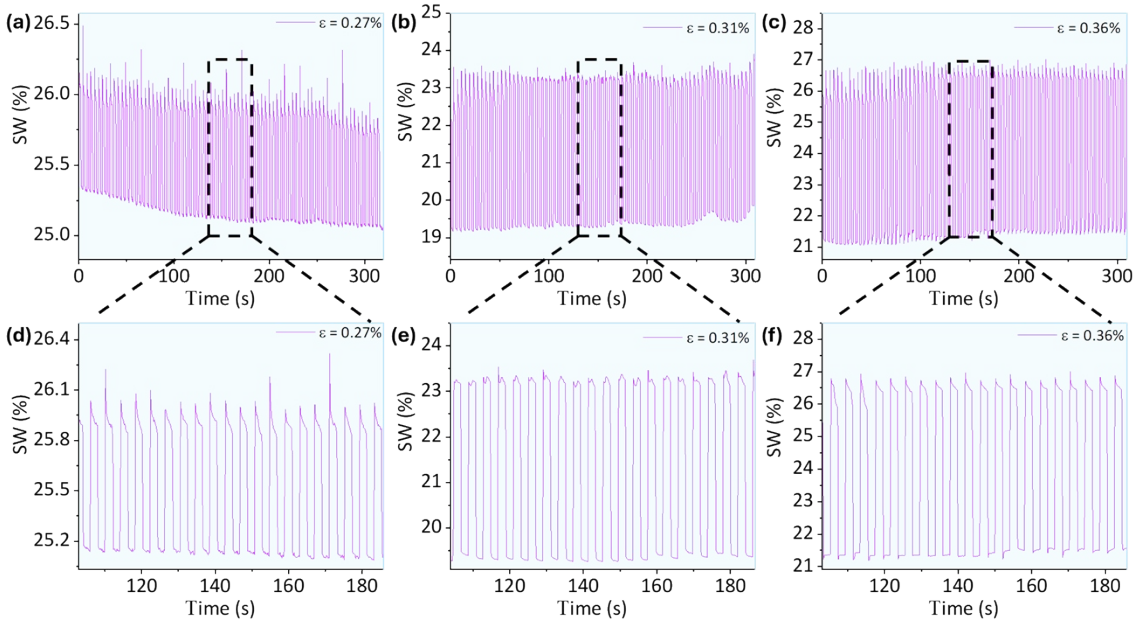

Fig. S9. The SW of the device altered across 155 cycles for the device with a PDMS curing agent to base ratio of 1:10, (a & d) displacement Δx of 16 µm (ε, 0.27%), (b & e) 19 µm (ε, 0.31%), and (c & f) 22 µm (ε, 0.36%).

The response speed of our device is quite impressive (t_{res}, 7 ms), though the actual response could potentially be even faster, as the measurements may be limited by the response associated with the x-y translation stage.

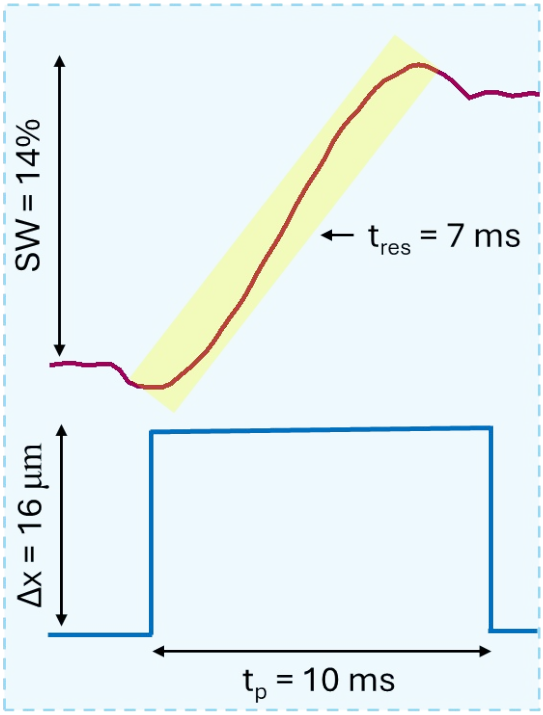

Fig. S10. The device showed a response in 7 ms (t_{res}) for the application of a 10 ms displacement pulse (t_p) of 16 µm amplitude (Δx).

However, the response speed of this PDMS composite-based device can be further improved by adjusting the elasticity of the PDMS matrix by fine-tuning the curing agent-to-base (C:B) ratio of the substrate, as more flexible substrates facilitate quicker response on strain application. Additionally, the thickness of the PDMS substrate can also be reduced to enhance response speed as a thin PDMS layer will reduce the time required for strain propagation.

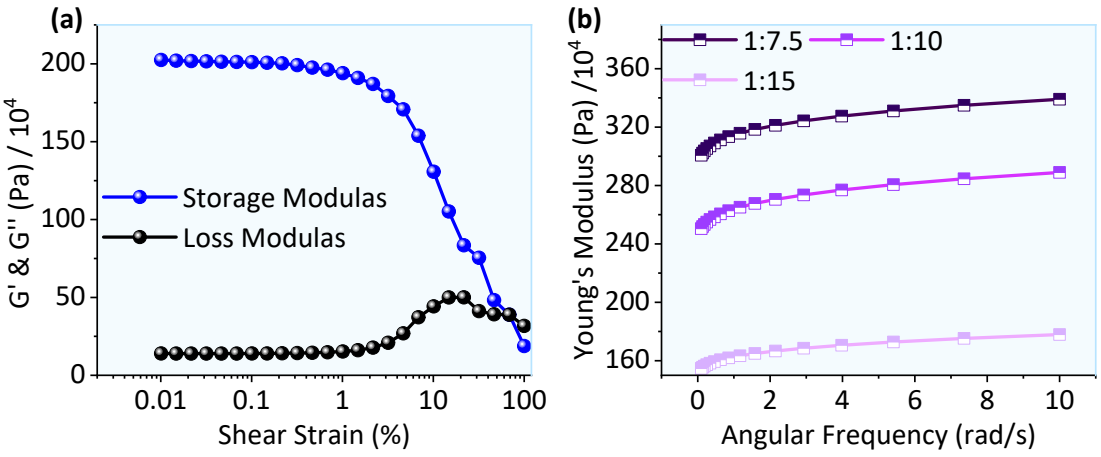

Fig. S11 (a) Variation of storage modulus (G′) and loss modulus (G′′) with shear strain. Up to 1% shear strain, the substrate remains in the linear viscoelastic region. The sample behaves elastically up until this point without deforming (C:B, 1:7.5). (b) Variation of Young's modulus (Y) with angular frequency for substrates with C:B as 1:7.5, 1:10, and 1:15. The increasing value of Y with decreasing curing agent concentration represents the less flexible nature of substrates for the device. Young's modulus was calculated using eqn:

$$Y = 2 (1+ \upsilon) G'$$

where Y is Young's Modulus, G′ is Storage Modulus, and υ is Poisson's ratio.

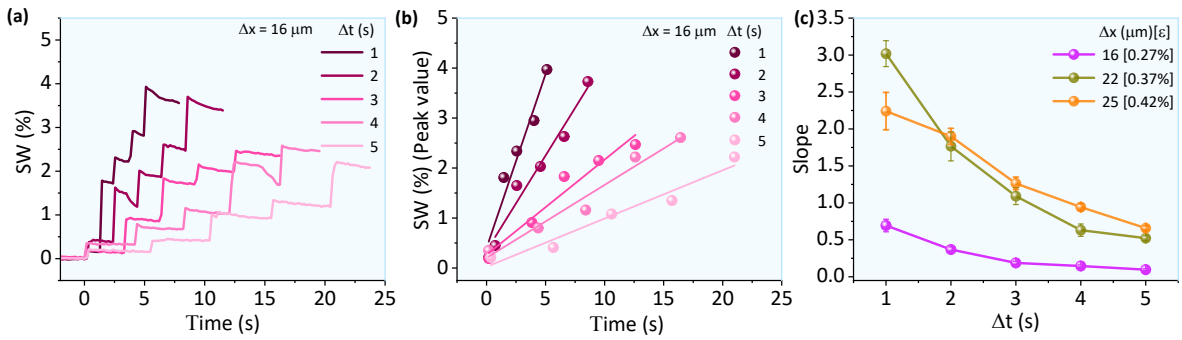

Fig. S12 (a) Change in resistance of D1 (C:B, 1:7.5) with varying time intervals of displacement pulses from 1 to 5 s (ε, 0.27%, Δx, 16 μm). (b) The peak resistance exhibits a linear relationship with time at different time intervals (c) Slope values obtained from the linear fitting in (b) plotted against each pulse time interval for three different ε, 0.27%, 0.37%, and 0.42%. The slopes represent a decreasing trend with pulse time interval (PPF behavior) and an increase with strain amplitude.